Coexistence of acute severe leukocytosis and anaplastic lymphoma kinase-positive histiocytic sarcoma, a rare entity with an unusual presentation: A case report

ERTUGRUL BAYRAM[1], UMUR ANIL PEHLIVAN[2], KIVILCIM EREN ERDOGAN[3], MEHMET TURKER[4], HAFIZE YALNIZ[5] and SEMRA PAYDAS[1]

[1]Department of Medical Oncology, Cukurova University Faculty of Medicine, Adana 01330, Turkey; [2]Department of Radiology, Baskent University Adana Dr. Turgut Noyan Application and Research Center, Adana 01240, Turkey; [3]Department of Pathology, Cukurova University Faculty of Medicine, Adana 01330, Turkey; [4]Department of Medical Oncology, Adana City Training and Research Hospital, Adana 01330, Turkey; [5]Department of Cardiovascular Surgery, Cukurova University Faculty of Medicine, Adana 01330, Turkey

Received November 21, 2023; Accepted July 9, 2024

DOI: 10.3892/ol.2024.14649

Abstract. Soft tissue sarcomas are rare cancers and most cases are metastatic at the time of diagnosis. Although the chances of survival are good with surgical treatment in the early stages, systemic treatment in the advanced stages is only associated with a survival duration of ~12 months. Alterations in the anaplastic lymphoma kinase (ALK) gene are becoming increasingly recognized as pan-cancer indicators in solid tumors. However, little is known regarding the molecular spectrum of ALK-positive histiocytosis. Molecular treatments, including ALK inhibitors, are potential treatment options. The present case report describes an aggressive ALK-positive soft tissue sarcoma with intracardiac metastases and severe leukocytosis responding to ALK inhibitors. The patient initially responded to crizotinib but required alectinib due to central nervous system progression. The patient has shown a near-complete response and remained stable for 2 years; however, there has been recent lymph node progression.

Introduction

Histiocytic sarcoma (HS) is a rare non-Langerhans histiocyte disorder that presents as unifocal or multifocal extranodal tumors. The diagnosis of HS can be difficult due to its rarity and histologic similarity to a number of other tumors (1). Diagnosis depends on the identification of morphological features and the appropriate use of immunohistochemistry (IHC) markers to validate the histiocytic lineage and exclude others (2). HS may be sporadic or clonally related to hematological malignancies, including follicular lymphoma or acute lymphoblastic leukemia (3). In addition, HS has been reported in patients with mediastinal germ cell tumors, such as malignant teratomas, suggesting a possible derivation of such tumors from pluripotent germ cells (4-6). However, only a few hundred such cases have been reported in the literature (7).

Crizotinib is a kinase inhibitor approved by the Food and Drug Administration for the treatment of anaplastic lymphoma kinase (ALK)-positive or c-ros oncogene 1 receptor kinase-positive patients with metastatic non-small cell lung cancer (NSCLC) (8). Since the first case of an inflammatory myofibroblastic tumor (IMT) with ALK rearrangement demonstrated a favorable response to crizotinib, it gradually became an off-label treatment for inoperable sarcomas with ALK fusions (4,5). However, to the best of our knowledge, whether single-agent therapy using crizotinib is optimal and whether the specific partner protein in ALK fusion variants affects the response of the tumor to crizotinib remains unknown (6). The present case report describes the response to ALK inhibitors of an aggressive ALK-positive soft tissue sarcoma with intracardiac metastases and severe leukocytosis.

Case report

Case report. A 27-year-old woman presenting with shortness of breath, palpitations and fatigue was admitted to the emergency department (July 2022; Cukurova University Medical Faculty Balcalı Hospital, Adana, Turkey). The patient had a fever of 38˚C and a pulse rate of 140 beats/min, their electrocardiogram demonstrated sinus tachycardia, and the blood gas test indicated hypoxia and hypocapnia. The white blood cell (WBC) count and hemoglobin levels were 55,000/μl and 10 g/dl, respectively (reference range, 48,000-108,000/μl and 14-18 g/dl, respectively). The patient also exhibited a high C-reactive protein level of 236 mg/l and hypoalbuminemia was detected in blood tests (32.79 g/l) (reference range,

Correspondence to: Dr Ertugrul Bayram, Department of Medical Oncology, Cukurova University Faculty of Medicine, Balcali, Mithat Ozhan 17, Saricam, Adana 01330, Turkey
E-mail: ertugrulbayram84@gmail.com

Key words: crizotinib, histiocytic sarcoma, leukocytosis, anaplastic lymphoma kinase

0-5 mg/l and 34-54 g/dl, respectively). Flow cytometry and ELISA methods were used and these data were obtained from medical records. Thoracic computed tomography revealed a mass ~11 cm in size located in the right hemithorax, causing a tumor thrombus that extended to the left atrium through the pulmonary veins (Figs. 1 and 2A), and these findings indicated lung and cardiac metastasis. Sputum culture and rapid antigen tests for specific infectious agents yielded negative results. A peripheral blood smear identified neutrophilic leukocytosis and a bone marrow biopsy indicated myeloid hyperplasia. The standard diagnostic procedure of the hospital includes JAK2 V617F mutation assessment (Allele-Specific PCR; data were obtained from medical records) when myeloproliferative disease is suspected. Since the JAK2 V617F mutation result was negative, which suggested that another ailment may exhibit comparable symptoms or that the disease had another etiology, further testing was conducted.

A mediastinal biopsy demonstrated spindle cells with orthochromatic and indistinct nucleoli. Neoplastic cells were arranged in fascicles, nests and sheets in the inflammatory and vascular backgrounds. IHC demonstrated no staining for HMB45, CD34, smooth muscle actin (SMA), S100, CD117, chromogranin, synaptophysin, CD56, transcription factor binding to IGHM enhancer 3 (TFE3) or mucin-4 (MUC-4).

Subsequently, the patient underwent a right middle lobectomy, and it was demonstrated that the tumor completely infiltrated the entire tissue sample obtained. Microscopic assessment revealed a spindled tumor mixed with inflammatory cells, and H&E initial biopsy indicated monotonous spindle cells with mild atypia accompanied by inflammatory cells. The H&E resection specimen exhibited oval round vesicular nuclei and abundant eosinophilic cytoplasm (Fig. 2B and C; data were obtained from medical records) and a barely malignant tumor. The case exhibited areas of stag horn vessels.

Immunostaining was performed for CD163, lysozyme, CD10, CD13, ALK, CD21, CD23, TFE3, Inhibin, CD4, STAT6, ETS transcription factor ERG (ERG), cytokeratin (Pan) (PanCK), epithelial membrane antigen (EMA), CD34, CD117 and myeloperoxidase (MPO). IHC revealed positivity for CD163 (Fig. 2D), lysozyme, CD10, CD13 and ALK. IHC for CD21, CD23, TFE3, Inhibin, CD4, STAT6, ERG, PanCK, EMA, CD34, CD117 and MPO was negative.

Translocation of EML4/ALK 2p23 was assessed using the Vysis ALK break-apart fluorescence *in situ* hybridization (FISH) probe kit (cat. no. 30-608916/R8; Abbott Laboratories) (Fig. 3). The combination of visceral crisis, dyspnea, high WBC count and the necessity for major surgery indicated an aggressive hematologic malignancy.

A positive clinical response was observed in the patient after treatment with 250 mg crizotinib, administered orally, twice a day. A decrease in the WBC count within 10 days of crizotinib treatment was observed (Fig. 4). However, 6 months later, the patient began to experience headaches and brain magnetic resonance imaging demonstrated a mass in the right frontal lobe [central nervous system (CNS) involvement; Fig. 5A and B]. After progression, liquid biopsy and next-generation sequencing (NGS) were performed, and the ALK p.I1171T mutation was detected. The patient was positioned on the Gamma Knife couch, with the head frame fixed in place to maintain the correct alignment. The Gamma Knife device delivered focused gamma rays to the targeted lesions. The treatment was typically performed in a single session, with each lesion receiving a precise dose of radiation according to the pre-established plan. Throughout the procedure, the patient was closely monitored to ensure stability and comfort. The medical team could communicate with the patient and make any necessary adjustments. Furthermore, 600 mg alectinib, administered orally, twice daily was prescribed because of an improved intracranial response (9). Although the patient tolerated alectinib for 2 years (Fig. 5C and D), the intra-abdominal lymph nodes progressed. NGS was performed again and a ALK p.I1171N mutation was detected and lorlatinib treatment (administered orally; 100 mg; once a day) was started. After the treatment, the patient was followed up with a haemogram and renal and liver tests every month, and no side effects were observed. The patient was planned to be followed up with PET CT after treatment and this will be done at 3-month intervals.

FISH. FISH was performed using paraffin-embedded tissue sections, which were fixed with 3% paraformaldehyde at room temperature for 10-20 min. The samples were permeabilized with a 0.1% pepsin solution (prepared from pepsin powder from Sigma-Aldrich; Merck KGaA) in 0.01 N HCl at 37˚C for 10 min. The sections were fixed with 3% paraformaldehyde at room temperature for 10 min. Selected paraffin blocks were sectioned into 4-μm-thick sections and mounted on positively charged slides. The sections were incubated overnight at 56˚C to ensure proper adhesion to the slides. Slides were deparaffinized by immersion in three changes of xylene for 10 min each. This was followed by dehydration in absolute ethanol (two changes; 5 min each) and air-drying to remove any residual solvent. Pre-treatment involved placing the slides in a heat-resistant container with deparaffinization pre-wash solution and incubating the slides at 80˚C. Each slide box contained 15 cc of distilled water and 150 μl of 1 mol HCl, and was incubated at 37˚C. After this step, the slides were washed in 2X SSC solution (two times; 3 min each) and passed through a graded ethanol series (70, 85 and 100%) for 3 min each, followed by air-drying (pre-hybridization). The hybridization buffer comprised 50% formamide, 10% dextran sulfate and 2X SSC solution. Before the probe was applied, the sections were incubated in hybridization buffer at 37˚C for 30 min. The probe (~1 ng/μl) was applied to the sections, and coverslips were placed over the sections. The slides were denatured at 73˚C for 5 min using a ThermoBrite device. The slides were then incubated at 37˚C for 16 h to allow hybridization. Post-hybridization, the slides were washed in a SSC solution at 73˚C for 3 min to remove any non-specifically bound probes. This was followed by an additional wash with SSC solution at room temperature for 2 min. The sections were counterstained with 10 μl DAPI at room temperature for 5-10 min and coverslipped. The slides were stored at -20˚C for 1 h before evaluation. The FISH slides were evaluated using a fluorescence microscope (Olympus BX61; Olympus Corporation). The slides were analyzed for the presence of specific signals indicating genetic abnormalities. Positive cases such as the present case were identified by the presence of break-apart signals, where the distance between red and green signals was at least twice the estimated signal diameter, or the presence of a single red signal in >15% of the tumor cells.

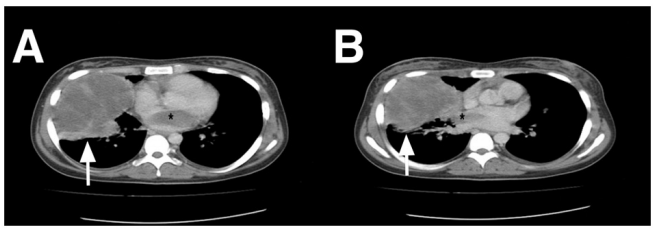


Figure 1. (A and B) Contrast-enhanced CT revealing a heterogeneous hypodense mass lesion (arrows) extending to the left atrium through the pulmonary veins (asterisks).

IHC. IHC was performed as part of the diagnosis and some specific experimental details were not available. Tissue slides were produced from surgical pathology formalin-fixed, paraffin-embedded neoplastic tissue samples. Paraffin-embedded tissues were fixed with 10% formaldehyde at 60-62˚C for 3 h. Paraffin-embedded tissue samples were cut into sections (2-4 μm thick) and mounted on positively charged slides. Tissue slides were pretreated with high pH heat-induced epitope retrieval using Cell Conditioning 1 solution, which is part of the VENTANA BenchMark ULTRA automated staining platform kit (Roche Diagnostics), at 60-62˚C for 88 min. Rehydration was performed using a descending alcohol series. The slides were incubated with primary antibodies against CD163 (10D6; 1:100; mouse monoclonal antibody; Cell Marque; Merck KGaA), ALK (ALK1; 1:100; mouse monoclonal antibody; Dako; Agilent Technologies, Inc.), lysosome (LAMP1; H4A3; 1:100; mouse monoclonal antibody; Abcam), CD23 (1:100; Liquid Mouse Monoclonal Antibody; Novocastra Laboratories Ltd.), CD4 (1:100; Novocastra Liquid Mouse Monoclonal Antibody; Novocastra Laboratories Ltd.), CD10 (1:100; Novocastra Liquid Mouse Monoclonal Antibody; Novocastra Laboratories Ltd.), CD21 (2G9; 1:100; Cell Marque; Merck KGaA), TFE3 (MRQ37; 1:100; rabbit monoclonal antibody; Cell Marque; Merck KGaA), STAT6 (EP325; 1:100; rabbit monoclonal antibody; Cell Marque; Merck KGaA), MPO (1:400; Cell Marque; polyclonal antibody; Merck KGaA), CD45 (2B11 & PD7/26; 1:200; mouse monoclonal antibody; Cell Marque; Merck KGaA), EMA (E29; 1:400; Cell Marque; Merck KGaA), ERG (EPR3864; rabbit monoclonal antibody; Roche Tissue Diagnostics; Roche Diagnostics, Ltd.), CD117 (YR145; 1:100; rabbit monoclonal antibody; Cell Marque; Merck KGaA) and CD34 (1:100; mouse monoclonal antibody; Novocastra Laboratories Ltd.) for 16 min at room temperature. Staining was visualized using an ultraView Universal DAB Detection Kit (Roche Diagnostics). IHC was performed on the automated Benchmark XT platform (Roche Tissue Diagnostics; Roche Diagnostics, Ltd.). The stained slides were assessed under an Olympus BX46 light microscope (Olympus Corporation).

NGS. Peripheral blood samples (10 ml each) were collected into biological specimen collection tubes. The circulating cell-free DNA (ccfDNA) was isolated using the Qiagen QIAamp Circulating Nucleic Acid Kit (cat. no. 55114; Qiagen, Inc.) with the aid of the Qiagen QIAvac 24 Plus vacuum system (cat. no. 19413; Qiagen, Inc.). After isolation, ccfDNA concentrations were measured using the Qubit 3.0 Fluorometer (cat. no. Q33216; Thermo Fisher Scientific, Inc.). The quality and integrity of the processed ccfDNA samples were verified using the Qubit 3.0 Fluorometer, which provides precise concentration measurements ensuring that samples meet the required thresholds for further processing. For sequencing, genomic DNA (gDNA) was extracted from formalin-fixed, paraffin-embedded (FFPE) tissue samples using the Qiagen GeneReader FFPE Kit (cat. no. 180134; Qiagen, Inc.) and the Qiagen QIAcube isolation device (cat. no. 9001794; Qiagen, Inc.). The DNA quality was confirmed using the Qubit 3.0 Fluorometer. Only samples with a gDNA concentration of at least 1.5 ng/μl proceeded to sequencing. The sequencing performed was NGS with paired-end reads of 150 nucleotides in length. The sequencing was carried out using the Illumina TruSeq DNA PCR-Free Library Prep Kit (cat. no. 20015960; Illumina, Inc.). The final library loading concentration was determined using the Qubit 3.0 Fluorometer, ensuring accurate and reliable measurements. The sequencing data were analyzed using the Illumina BaseSpace Sequence Hub (version 5.0; Illumina, Inc.), accessible at Illumina BaseSpace. This software provided comprehensive tools for data analysis, including alignment, variant calling and annotation, allowing for detailed insights into the genomic data obtained from the samples.

Discussion

The first pathological diagnosis in the present case was IMT. IMT is a rarely metastasizing tumor which is composed of myofibroblastic and fibroblastic cells accompanied by an infiltrate of plasma cells, lymphocytes and eosinophils (6). However, further assessment demonstrated that the tumor was composed of spindle cells with orthochromatic nuclei and indistinct nucleoli. Neoplastic cells were arranged in fascicles, nests and sheets in the inflammatory and vascular background. The neoplastic cells exhibited malignant features with enlarged nuclei, frequent and atypical mitosis with necrosis, which is different from IMT. Furthermore, the tissue was demonstrated to be diffusely positive for CD163, which is not observed in IMT (5). In IMT, one or more patterns are often observed in a single tumor. The spindle cells contain vesicular nuclei and small nucleoli. Necrosis is uncommon and mitotic activity is generally low. Immunohistochemically, the neoplastic cells display variable staining for SMA, desmin and calponin, whereas ALK positivity is observed in 50-60% of IMTs (7). In the present case, a diagnosis of IMT was initially considered because of the presence of low-grade spindle cells mixed with inflammatory cells; however, malignancy was demonstrated by the presence of enlarged nuclei, frequent and atypical mitosis, and necrosis, distinguishing it from IMT. These features include abnormal large nuclei, high mitotic activity with atypical figures, and areas of cell death, which are indicative of aggressive tumor behavior and differentiate it from IMT, and IMT was excluded.

Although HS is diagnosed at all ages, it is most common among adults. The median patient age is 63 years (range, 18-96 years) according to the US Surveillance, Epidemiology, and End Results database, which covers 159 cases of HS. These 159 cases include 99 men and 60 women (10). In the

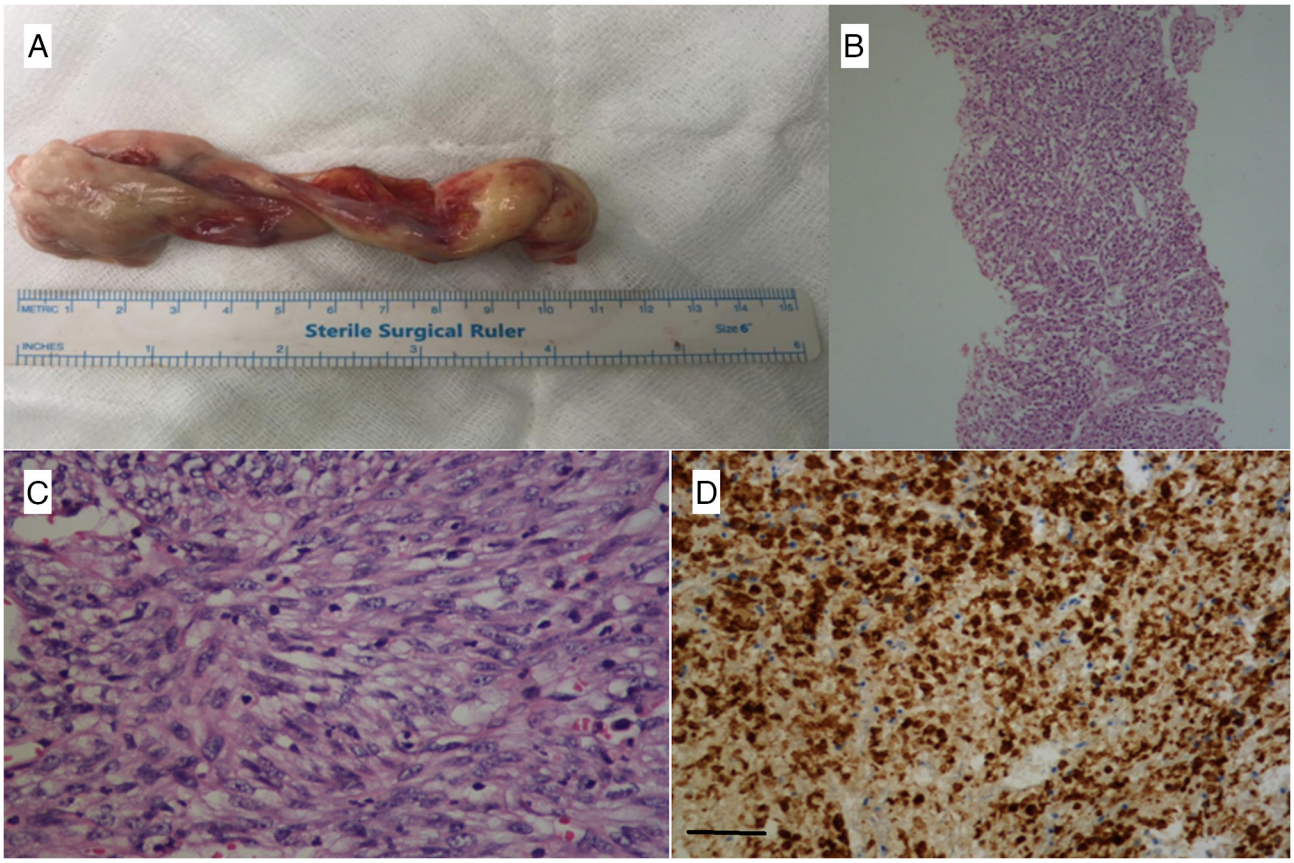


Figure 2. (A) Specimen macroscopy (tissue samples obtained from surgical resection). (B) H&E initial biopsy showing monotonous spindle cells with mild atypia accompanied by inflammatory cells. Magnification, x40. (C) H&E resection specimen showing oval round vesicular nuclei and abundant eosinophilic cytoplasm. Around the tumor cells, small vessels and inflammatory cells were observed. Magnification, x200. (D) Diffuse CD163 positivity. Scale bar, 60 μm.

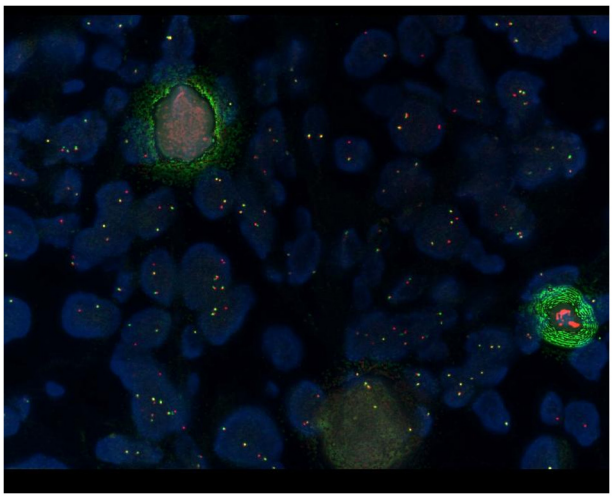


Figure 3. EML4/ALK. Four gene regions were analyzed, 24/100 cells were 2p23 translocated and the cut off was 15%.

present case, the patient was 27 years old, and thus, younger than the median patient age.

Histiocytic neoplasms are derived from macrophages, dendritic cells or histiocytes. These neoplasms are rare and account for <1% of the tumors present in the lymph nodes or soft tissues. HS is commonly present at extranodal sites. The tumor cells have oval-round vesicular nuclei and abundant eosinophilic cytoplasm (11). In the present case, reactive inflammatory cells were observed in the background, mimicking inflammatory neoplasms such as IMTs. Other differential diagnoses included solitary fibrous tumors, vascular neoplasms, myeloid sarcomas, interdigitating dendritic cell sarcomas, follicular dendritic cell sarcomas and inflammatory pseudotumor-like follicular/fibroblastic dendritic cell sarcomas, which were all excluded by negative immunostaining for STAT6, CD34, ERG, MPO, S100, CD21 and CD23, respectively (12).

The pathogenesis of HS is unclear; it is not a true sarcoma but is derived from cells of the monocyte/macrophage system. The clinical presentation of HS varies, depending on the organ involved. Solitary involvement of the lymph nodes is observed in <20% of cases (13). Furthermore, cytopenia is observed in one-third of cases and hemophagocytosis is observed in a few cases (5-7). The patient in the current case report presented with severe neutrophilic leukocytosis. The WBC count rapidly decreased with specific treatment. No patients with HS and leukocytosis were identified in the literature. A biopsy of the tumor demonstrated an infiltrative process with a diffuse growth pattern and effacement of the normal architecture (7). IHC demonstrated lysozyme and CD163 positivity and negative results for T and B cell markers, myeloid cell markers CD1a and S100, and epithelial markers. HS must be distinguished from other histiocytic and dendritic cell disorders, metastatic solid or hematopoietic neoplasms, primary familial

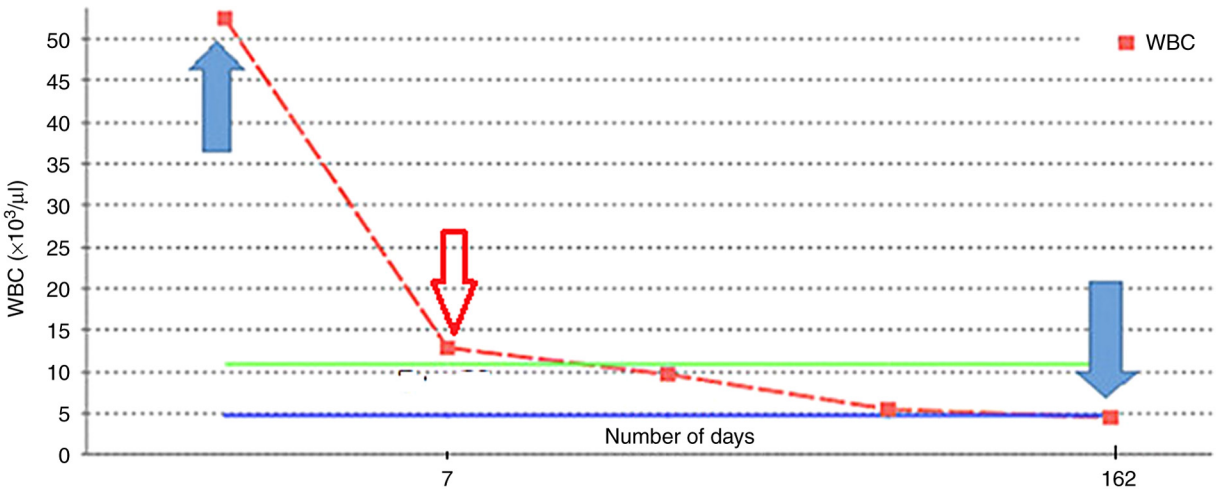


Figure 4. Schematic representation of the response of WBC values to treatment with alectinib and crizotinib. There are 7 days between the first blue arrow and the red arrow and 162 days between the two blue arrows. The green line emphasizes the weekly change and the blue line emphasizes the change of ~5 months. WBC, white blood cell.

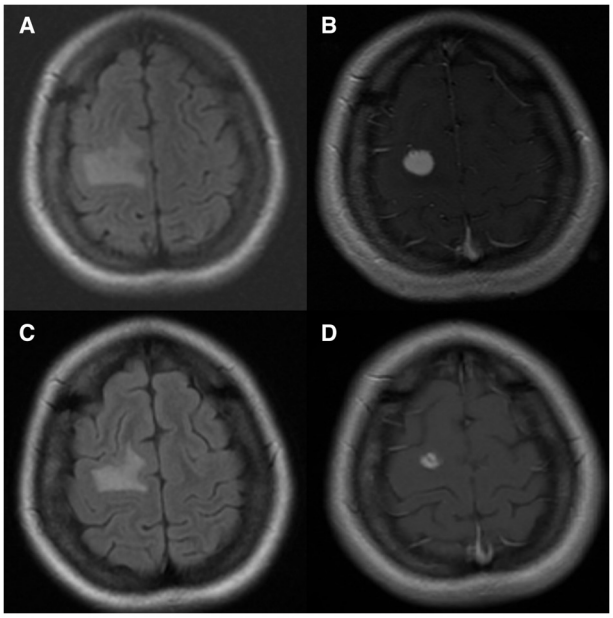


Figure 5. (A and B) Pre-treatment FLAIR and post-contrast T1-weighted images showing mass, and surrounding edema in the right frontal lobe. (C and D) Post-treatment FLAIR and post-contrast T1-weighted images reveal that reduced mass size and surrounding edema after alectinib treatment. FLAIR, fluid-attenuated inversion recovery.

lymphohistiocytic disorders and acquired causes of hemophagocytic macrophage activation syndrome. The present case was diagnosed using resected tissues and multiple immunohistochemical stains, including CD163, lysozyme, CD10, CD13, ALK, CD21, CD23, TFE3, Inhibin, CD4, STAT6, ERG, PanCK, EMA, CD34, CD117 and MPO. Additionally, FISH analysis confirmed ALK p.I1171N mutation positivity.

Severe leukocytosis was a prominent laboratory finding in the present case, suggesting myeloproliferative neoplasia (14). However, there was no evidence of this entity, suggesting that leukocytosis was associated with HS. The positive response to treatment with ALK inhibitors suggests that leukocytosis was associated with HS (15). Leukocytosis associated with HS (total WBC count in the blood, 25.57x10^9/l) has, to the best of our knowledge, only been reported in 1 case of a 84-year-old male patient (16).

ALK-positive sarcoma is predominantly observed in pediatric or middle-aged patients. In a previous study of a cohort of 33 cases, only 2 patients were aged >60 years. IMT and its variant epithelioid IMTs comprised the majority of cases, accounting for 78.8% (26/33) of cases (17). Although limited by sample size, a pooled analysis reported a 86.7% efficacy of crizotinib in ALK-positive sarcomas or sarcomatoid malignancies, with equal effectiveness in both adult and pediatric patients (8). Furthermore, mutations in the ALK fusion gene cause resistance to crizotinib in ~30% of cases (18). Second-generation ALK-tyrosine kinase inhibitors (TKIs), including ceritinib, brigatinib and alectinib, are usually effective at later stages, and the advantage of these drugs is intracranial tumor control (9).

A previous case series reported the efficacy of ALK-TKIs, including alectinib, a second-generation ALK-TKI, across a number of tumor types and fusion partners in patients with advanced ALK-rearranged, solid tumors other than NSCLC (10,11). Previous studies assessing ALK-positive histiocytosis (Table I) (15), HS and parotid gland adenocarcinoma have reported the efficacy of alectinib as a first- or second-line treatment (12-14). The responses of cases varied, with some patients experiencing stable or regressive disease for several years. Treatments included ALK inhibitors such as alectinib, lorlatinib and ceritinib, along with surgery and radiotherapy. A total of 67 cases were submitted to the accessory cell and histiocytic neoplasms session at the European Association of Haematopathology/Society in Hematopathology workshop 2016. From this, 12 cases had HS and 5 of these cases were reported to have the BRAF V650E mutation, which is a targetable somatic genetic change. However, no cases of ALK rearrangements were noted among these cases (13). Additionally, 1 patient with disseminated histiocytosis was reported to be ALK-positive. This patient showed partial recovery after treatment with alectinib and a response duration of >7 months (15).

Table I. Histiocytosis cases with EML4-ALK fusion or on alectinib therapy (15).

First author/s, year	Patient sex, age (years)	Site of disease	Targetable mutations	Treatment	Response	(Refs.)
Kemps *et al*, 2022	M, 17	Lung	EML4-ALK	N/A	Lost to follow-up	(15)
	F, 51	CNS, bone, lung	EML4-ALK	Alectinib for 16 months, followed by lorlatinib for 14 months and then ceritinib for 7 weeks, followed by antalgic radiotherapy of two metastases and chemotherapy	Alive with stable disease (3 years)	
	F, 4	CNS/PNS, bone, lung, liver, lymph node, breast, pancreas	EML4-ALK	Alectinib	Alive with stable bone lesions on MRI; other lesions regressed (2 years)	
	F, 19	Soft tissue: A yellow nodule in the left main bronchus	KIF5B-ALK	Surgery	Alive with no disease (17 years)	
	F, 28	CNS/PNS, bone	KIF5B-ALK	Alectinib	Alive with regressive disease (9 months)	
Present study	F, 27	Lung, cardiac metastasis, CNS	EML4-ALK	Alectinib	Near-complete response for 2 years, with the exception of lymph node metastasis.	-

ALK, anaplastic lymphoma kinase; CNS, central nervous system; F, female; M, male; N/A, not applicable; PNS, peripheral nervous system.

Solitary fibrous tumor is a fibroblastic tumor, which is characterized by a prominent branching thin-walled dilated vasculature (5). The present case exhibited areas of stag horn vessels; however, STAT6 was negative based on IHC. Vascular neoplasms, particularly epithelioid hemangioma and epithelioid hemangioendothelioma, exhibit features similar to the present case. They typically exhibit voluminous cytoplasm and enlarged epithelioid cells (19). However, there are distinguishing characteristics between the two. Epithelioid hemangioma exhibits well-formed vascular channels, whereas epithelioid hemangioendothelioma is typically associated with a myxochondroid stroma (20,21). The differential diagnosis is made by IHC, with negativity of vascular markers observed in the present case.

Another differential diagnosis is myeloid sarcoma, which is a malignant tumor composed of myeloblasts occurring at a site other than the bone marrow. The myeloblasts mimic carcinoma, lymphoma or sarcoma (22). Differential diagnosis between myeloid sarcoma and the present case was challenging. However, the CD56, CD34, CD117 and MPO negativity, and CD163 and CD13 positivity were helpful. Differential diagnosis between myeloid sarcoma and the present case was challenging due to overlapping histological features. However, immunohistochemical staining provided valuable insights. The negativity for CD56, CD34, CD117 and MPO was particularly helpful in ruling out myeloid sarcoma, as these markers are typically expressed in myeloid lineage cells (23). On the other hand, the positivity for CD163 and CD13 supported the diagnosis of the present case, as these markers are more commonly associated with histiocytic and monocytic lineage (2), aligning with the characteristics of the tumor. Interdigitating dendritic cell sarcoma is another differential diagnosis, and is composed of whorls of large, pleomorphic cells with abundant pale cytoplasm with inflammatory infiltrate (24). However, the IHC results demonstrated that the present case was negative for S100, CD45 and EMA. S100 is a marker commonly associated with neural and melanocytic tumors, and thus, its negativity suggests that the tumor was unlikely to originate from these lineages (24,25). CD45, also known as leukocyte common antigen, is a marker for hematopoietic cells, particularly lymphoid tissue. Its absence indicates that the tumor was not of lymphoid origin (26). Furthermore, follicular dendritic cell sarcoma is composed of spindled cells with dispersed chromatin, small nucleoli and eosinophilic cytoplasm accompanied

by inflammatory cells. The differential diagnosis was made by IHC (21), where CD21 and CD23 were negative. Furthermore, no staining was detected for HMB45, CD34, SMA, S100, CD117, chromogranin, synaptophysin, CD56, TFE3 and MUC-4 in the present case. In a more detailed IHC analysis, positive results were obtained for CD163, lysozyme, CD10, CD13 and ALK. However, negative results were obtained for CD21, CD23, TFE3, Inhibin, CD4, STAT6, ERG, PanCK, EMA, CD34, CD117 and MPO. Furthermore, EML4/ALK 2p23 translocation was detected. These findings indicate that certain different diagnoses have been excluded in the present case, confirming its association with ALK translocation, which characterizes an aggressive form of HS. Therefore, the aforementioned differential diagnoses were excluded based on the negative immunostaining results and contributed to the identification of HS in the case (18,27,28).

The present case illustrates three findings. First, although both HS and leukocytosis are rare and complex conditions that require separate treatments, they were successfully controlled in the patient. The patient presented with severe neutrophilic leukocytosis and responded to first-line crizotinib; however, alectinib was administered because of progression in the CNS.

To the best of our knowledge, this is the first reported case of ALK-rearranged p.I1171N-mutated HS with cardiac and CNS involvement that rapidly responded to alectinib, an ALK-TKI.

ALK-TKI resistance generally develops via ALK-dominant second-step mutations and non-dominant mechanisms (15). This mutation (p.I1171N) may be responsible for resistance to first-line crizotinib treatment. Frequent crizotinib resistance and low CNS efficacy in ALK-positive patients are a challenge for clinicians (28,29). Therefore, treatment with alectinib, a more effective second-generation TKI that is also effective on the CNS (16), was initiated and continued as the response persisted.

Resistance to first-line therapy is considered a novel entity among ALK-positive non-Langerhans histiocytic diseases (11). The present case report offers a rational treatment analysis of a problematic case of HS diagnosed in a young patient presenting with severe leukocytosis with an aggressive course and important organ metastases specifically involving the heart (cardiac metastases) and lungs (lung metastases). The patient also had a limited response to chemotherapy treatments and poor prognosis and is rare. The rarity is highlighted by the young age, severe leukocytosis and aggressive course of the disease with metastases to critical organs such as the heart and lungs. Additionally, while ALK fusions or rearrangements are reported in both solid and hematological tumors, the specific presentation of HS with these characteristics is uncommon in the literature. A number of notable cases of both solid and hematological tumor types with ALK fusions or rearrangements have been reported in the literature (3,14-17). This emphasizes the necessity of a multidisciplinary approach for evaluating ALK-positive histiocytosis with a solid component. Overall, the diagnosis of such sarcomas can be complex, and combination of histological, immunohistochemical and genetic analyses is required.

In conclusion, the present case illustrates the importance of the clinical integration of the molecular profile of the tumor for patient-specific treatment selection. Treatment selection based on the specific molecular characteristics of a patient can improve treatment success. Therefore, broad molecular profiling and clinical applications of these technologies can help patients achieve improved outcomes in the future.

Acknowledgements

Not applicable.

Funding

No funding was received.

Availability of data and materials

The data generated in the present study may be requested from the corresponding author.

Authors' contributions

EB contributed to the conception of the study, as well as to the literature search for related studies. EB, UAP, KEE, MT, HY and SP were involved in the writing of the manuscript, and in the analysis and interpretation of the patient data. EB, UAP and KEE contributed to the literature review, study design, revision of the manuscript and the processing of the figures. EB and UAP confirm the authenticity of all the raw data. All authors have read and approved the final version of the manuscript.

Ethics approval and consent to participate

Not applicable.

Patient consent for publication

The patient provided written consent for the publication of the present report.

Competing interests

The authors declare that they have no competing interests.

References

1. Ansari J, Naqash AR, Munker R, El-Osta H, Master S, Cotelingam JD, Griffiths E, Greer AH, Yin H, Peddi P and Shackelford RE: Histiocytic sarcoma as a secondary malignancy: Pathobiology, diagnosis, and treatment. Eur J Haematol 97: 9-16, 2016.
2. Hung YP and Qian X: Histiocytic sarcoma. Arch Pathol Lab Med 144: 650-654, 2020.
3. Egan C, Lack J, Skarshaug S, Pham TA, Abdullaev Z, Xi L, Pack S, Pittaluga S, Jaffe ES and Raffeld M: The mutational landscape of histiocytic sarcoma associated with lymphoid malignancy. Mod Pathol 34: 336-347, 2021.
4. Butrynski JE, D'Adamo DR, Hornick JL, Dal Cin P, Antonescu CR, Jhanwar SC, Ladanyi M, Capelletti M, Rodig SJ, Ramaiya N, *et al*: Crizotinib in ALK-rearranged inflammatory myofibroblastic tumor. N Engl J Med 363: 1727-1733, 2010.
5. Gambacorti-Passerini C, Orlov S, Zhang L, Braiteh F, Huang H, Esaki T, Horibe K, Ahn JS, Beck JT, Edenfield WJ, *et al*: Long-term effects of crizotinib in ALK-positive tumors (excluding NSCLC): A phase 1b open-label study. Am J Hematol 93: 607-614, 2018.
6. International Agency for Research on Cancer (IARC): Soft tissue and bone tumours. Vol 3. IARC, Lyon, France, 2020.

7. Sethi B, Pai T, Allam A and Epari S: Anaplastic lymphoma kinase-positive pulmonary inflammatory myofibroblastic tumor with sarcomatous morphology and distant metastases: An unusual histomorphology and behavior. Indian J Pathol Microbiol 58: 509-512, 2015.
8. Wang L and Wang W: Safety and efficacy of anaplastic lymphoma kinase tyrosine kinase inhibitors in non-small cell lung cancer (Review). Oncol Rep 45: 13-28, 2021.
9. Zou Z, Xing P, Hao X, Wang Y, Song X, Shan L, Zhang C, Liu Z, Ma K, Dong G and Li J: Intracranial efficacy of alectinib in ALK-positive NSCLC patients with CNS metastases-a multi-center retrospective study. BMC Med 20: 12, 2022.
10. WHO: Classification of tumours editorial board. Soft tissue and bone tumours. Lyon (France): International agency for research on cancer. Journal 3: 104, 2020.
11. Go RS, Jacobsen E, Baiocchi R, Buhtoiarov I, Butler EB, Campbell PK, Coulter DW, Diamond E, Flagg A, Goodman AM, *et al*: Histiocytic neoplasms, version 2.2021, NCCN clinical practice guidelines in oncology. J Natl Compr Cancer Netw 19: 1277-1303, 2021.
12. Swerdlow SH, Campo E, Harris NL, Jaffe ES, Pileri SA, Stein H and Thiele J: WHO classification of tumours of haematopoietic and lymphoid tissues. International agency for research on cancer Lyon, 2008.
13. Picarsic J and Jaffe R: Pathology of histiocytic disorders and neoplasms and related disorders. In: Histiocytic disorders. Abla O and Janka G (eds). Springer International Publishing, Cham, pp3-50, 2018.
14. Yogarajah M and Tefferi A: Leukemic transformation in myeloproliferative neoplasms: A literature review on risk, characteristics, and outcome. Mayo Clin Proc 92: 1118-1128, 2017.
15. Kemps PG, Picarsic J, Durham BH, Hélias-Rodzewicz Z, Hiemcke-Jiwa L, van den Bos C, van de Wetering MD, van Noesel CJM, van Laar JAM, Verdijk RM, *et al*: ALK-positive histiocytosis: A new clinicopathologic spectrum highlighting neurologic involvement and responses to ALK inhibition. Blood 139: 256-280, 2022.
16. Reddivari AKR, Mehta P and Janapala US: Rare presentation of a rare tumor: Histiocytic sarcoma. Cureus 12: e7770, 2020.
17. Solomon BJ, Mok T, Kim DW, Wu YL, Nakagawa K, Mekhail T, Felip E, Cappuzzo F, Paolini J, Usari T, *et al*: First-line crizotinib versus chemotherapy in ALK-positive lung cancer. N Engl J Med 371: 2167-2177, 2014.
18. Xu X, Li H, Peng K, Yu Y, Chen L, Fang Y, Sun Y, Hou Y and Liu T: ALK-G1269A mutation in epithelioid inflammatory myofibroblastic sarcoma after progression on crizotinib: A case report. Oncol Lett 17: 2370-2376, 2019.
19. Shon W and Billings SD: Epithelioid vascular tumors: A review. Adv Anat Pathol 26: 186-197, 2019.
20. Luzar B and Calonje E: Update on cutaneous epithelioid vascular tumours. Diagnostic Histopathology 24: 273-287, 2018.
21. Folpe AL: Vascular tumors of intermediate malignancy: An update. Hum Pathol 147: 114-128, 2024.
22. Magdy M, Karim NA, Eldessouki I, Gaber O, Rahouma M and Ghareeb M: Myeloid sarcoma. Oncol Res Treat 42: 224-229, 2019.
23. Thalhammer-Scherrer R, Mitterbauer G, Simonitsch I, Jaeger U, Lechner K, Schneider B, Fonatsch C and Schwarzinger I: The immunophenotype of 325 adult acute leukemias: Relationship to morphologic and molecular classification and proposal for a minimal screening program highly predictive for lineage discrimination. Am J Clin Pathol 117: 380-389, 2002.
24. Xue T, Jiang XN, Wang WG, Zhou XY and Li XQ: Interdigitating dendritic cell sarcoma: Clinicopathologic study of 8 cases with review of the literature. Ann Diagn Pathol 34: 155-160, 2018.
25. Szumera-Ciećkiewicz A, Bosisio F, Teterycz P, Antoranz A, Delogu F, Koljenović S, van de Wiel BA, Blokx W, van Kempen LC, Rutkowski P, *et al*: SOX10 is as specific as S100 protein in detecting metastases of melanoma in lymph nodes and is recommended for sentinel lymph node assessment. Eur J Cancer 137: 175-182, 2020.
26. Tuffaha MSA, Guski H and Kristiansen G: Markers and immunoprofile of lymphoid neoplasms. In: Immunohistochemistry in tumor diagnostics. Springer International Publishing, Cham, pp207-250, 2023.
27. Facchetti F, Simbeni M and Lorenzi L: Follicular dendritic cell sarcoma. Pathologica 113: 316-329, 2021.
28. Russo A, Franchina T, Ricciardi GRR, Ferraro G, Scimone A, Bronte G, Russo A, Rolfo C and Adamo V: Central nervous system involvement in ALK-rearranged NSCLC: promising strategies to overcome crizotinib resistance. Expert Rev Anticancer Ther 16: 615-623, 2016.
29. Nelson TA and Wang N: Targeting lung cancer brain metastases: A narrative review of emerging insights for anaplastic lymphoma kinase (ALK)-positive disease. Transl Lung Cancer Res 12: 379-392, 2023.

Copyright © 2024 Bayram et al. This work is licensed under a Creative Commons Attribution-NonCommercial-NoDerivatives 4.0 International (CC BY-NC-ND 4.0) License.